Optical Dipole Noise of Two-Level Atoms

A. M. Bacon, H. Z. Zhao, L. J. Wang,* and J. E. Thomas
Physics Department, Duke University, Durham, North Carolina 27708-0305
(Received 16 December 1994; revised manuscript received 24 April 1995)

We measure phase-dependent optical noise spectra for a simple system: long-lived coherently driven two-level atoms in an atomic beam. Very different noise spectra are measured for radiation which is in phase and out of phase with the driving field. The spectra and corresponding analysis afford clear insights into the roles played by three distinct sources of atomic noise. The measured noise spectra are in good agreement in magnitude and shape with results of a quantum treatment using no free parameters.

PACS numbers: 42.50.Lc, 32.80.–t

Optical dipole fluctuations play an important role in diverse physical phenomena. They limit the signal to background ratio that can be obtained in spectroscopic experiments, and hence limit the accuracy of atomic clocks [1]. In laser cooling and in optical traps, optical dipole fluctuations cause momentum diffusion, which determines the minimum temperature that can be obtained [2]. Dipole fluctuations also limit the amount of squeezing that can be obtained in atomic systems [3,4]. Despite the many theoretical and experimental studies of noise in radiating atomic systems [5], a complete physical picture of the distinct sources of atom noise has not been obtained. Hence, a detailed study of optical dipole fluctuations in a simple radiating system is of fundamental interest and of pedagogical value.

In this Letter, we report measurements of phase-dependent optical noise spectra for a particularly simple system: long-lived coherently driven two-level atoms in an atomic beam. We use atoms with a radiative lifetime long compared to the transit time of the atoms across the driving laser fields, so that noise spectra can be analyzed in terms of a simple fluctuating Bloch vector picture. Very different noise spectra are measured for radiation which is in phase or out of phase with the driving field. The spectra and corresponding analysis afford clear insights into the roles played by three distinct sources of atomic noise: phase-independent spontaneous emission noise, phase-dependent Bloch vector projection noise, and phase-dependent mean dipole Poisson noise. The first two noise sources arise from quantum fluctuations in the optical dipole moment of single atoms [6], while the last source arises from fluctuations in the number of radiating atomic dipoles. Remarkably, the phase-dependent part of the latter noise source can exactly cancel that of the former contribution in some cases.

Noise in the optical field radiated by atoms has been studied previously in short-lived systems [7]. Phase-dependent noise has been observed in the intensity of a probe beam transmitted through sodium vapor by Maeda *et al.* [4]. The noise spectrum of the transmitted probe field for a pumped, optically thick vapor has been studied recently by Kauranen *et al.* [8]. This work has elucidated the role of vacuum sideband coupling and gain in probe noise spectra.

The present experiments, Fig. 1, employ a 1 cm wide supersonic Yb beam which crosses two continuous laser field regions. The 556 nm $^1S_0 \rightarrow {}^3P_1$ transition of ^{174}Yb forms a two-level system comprising the $J = 0$ and the $J = 1, M = 1$ state with a radiative lifetime of 875 ns. Most of the Doppler shifts of the diverging supersonic beam are canceled by applying a magnetic field gradient along the laser propagation direction. This greatly enhances the intensity of the radiation field and

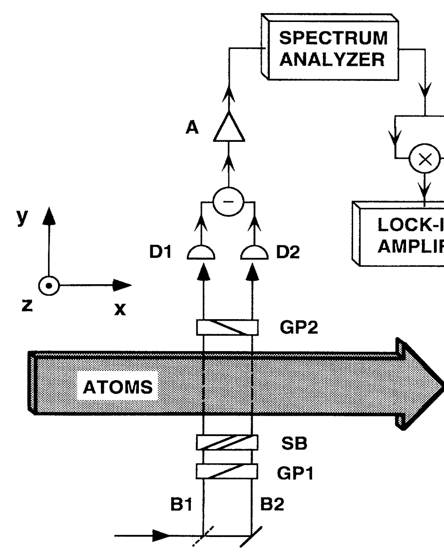

FIG. 1. Experimental scheme. Two identical preparation beams, B1 and B2, are polarized by GP1 in the **x**-**z** plane. A Babinet-Soleil compensator SB controls the relative phase between the **x**- and **z**-polarized field components. The total fields emerging from the sample are projected onto polarizer GP2. The field intensities are measured by photodiodes D1 and D2, where the output currents are subtracted. The technical noise in the difference signal subtracts while the quantum noise adds, because the two preparation beams are generated with a beam splitter and interact with independent atoms. Lock-in detection of the squared spectrum analyzer output voltage subtracts electronic noise in real time and measures the mean square optical noise on a linear scale.

 0031-9007/95/75(7)/1296(4)$06.00

simplifies data analysis, by permitting resonant excitation of the entire atomic volume by the driving field [9].

In each interaction region, atoms cross a continuous laser field that is polarized in the **x-z** plane by a glan prism GP1. Only the **x** component $\mathcal{E}_x$ interacts with the atoms, due to an applied Zeeman field. The relative phase between the **z** and **x** components is determined by a Babinet-Soleil compensator SB. The polarizer GP2 defines a local oscillator field $\mathcal{E}_{\mathrm{LO}}$, which is the net transmitted laser field. The axis of GP2 is oriented at 45° to the **z** axis, so that the **x**-polarized radiation field of the atoms is mixed with $\mathcal{E}_{\mathrm{LO}}$. Varying the phase of the compensator SB adjusts the relative phase ϕ between the driving field and the net local oscillator field; this allows measurement of noise spectra for in-phase and out-of-phase quadrature signals.

One important feature of the experiments is the subtraction of signals from the two interaction regions to measure quantum noise in the quadrature signals. Using this method, the technical noise in the local oscillator subtracts. This method also subtracts the excess noise in the nonvanishing quadrature signal [10], in contrast to homodyne detection with a beam splitter [11]. This feature is important in the present experiments because the quadrature signal is large enough that the excess noise would dominate the quantum noise signals of interest. In contrast to the technical noise which subtracts, the quantum noise from the two regions adds. This is due to the fact that the quantum fluctuations in the two radiating regions are independent, as the optical fields are generated with a beam splitter and interact with independent atoms.

Subtraction of signals from the interaction regions is implemented using diode detectors (EG&G FFD-040B) to monitor the signal fields transmitted through the projection polarizer. The detector outputs are subtracted and converted to a voltage by a low-noise transimpedance amplifier (Comlinear CLC 425, $R = 10\ \mathrm{k}\Omega$). Noise voltage signals from the amplifier are measured with a spectrum analyzer (HP 8553B).

Another important feature of the experiments is the direct measurement of the mean square optical noise voltage, i.e., the noise power spectrum, on a linear scale with high sensitivity. With this system, the atom contributions to the noise spectra are readily isolated from the shot noise and electronic noise contributions. This technique is implemented by squaring the analog voltage output of the spectrum analyzer using a low-noise multiplier (Analog Devices AD-534K). The output of the multiplier then is fed to a lock-in amplifier (SR 850-DSP), which subtracts the mean square noise signals obtained with the laser fields on and off. In this way, the mean square electronic noise is subtracted in real time, and the lock-in output is proportional to the mean square optical noise voltage [12].

As a calibration of the detection system, the mean square shot noise voltage is measured. In this case, the lock-in output scales linearly with the total power incident on the balanced detectors from 6 mW down to 2 μW. The measured slope agrees with predictions based on shot noise, the system gain factors, and the detector efficiency to better than 10% [13].

Atomic dipole noise contributions to the optical noise spectra are isolated by subtracting the shot noise contribution. First, the on-resonance transmitted power P is measured with a power meter. Then, with the laser off resonance, the power is reset to P and the lock-in output is measured; this determines the shot noise contribution to the measured spectrum.

Measured optical dipole noise spectra for radiation in phase with the driving field ($\phi = 0$) and out of phase with the driving field ($\phi = \pi/2$) are shown in Fig. 2. The baseline is not adjusted after subtraction of the shot noise. The dipole noise spectral density has been divided by the measured shot noise spectral density (V^2/Hz) for 1 mW of total power.

The measured phase-dependent noise spectra exhibit a number of interesting features. The in-phase spectrum appears as a broad peak centered near the Rabi frequency of the driving field, and exhibits a local minimum near 2.5 MHz. By contrast, the out-of-phase spectrum is centered at zero frequency, and is small near the Rabi sidebands. The out-of-phase noise approaches zero at high frequency, and it exceeds the in-phase noise at low frequency. At 3 MHz, the in-phase and out-of-phase spectra cross. At this frequency, the phase-dependent noise vanishes, leaving only the phase-independent contribution. Finally, it is interesting to note that the average of the in-phase and out-of-phase spectra is equivalent to the measurement of the fluorescence spectrum, with spectral resolution limited by the transit time across the local oscillator. The average of the measured noise spectra exhibits peaks centered at zero frequency and near the Rabi sidebands, similar to a Mollow spectrum [14].

The features of the measured noise spectra can be understood from the decay-free operator optical Bloch

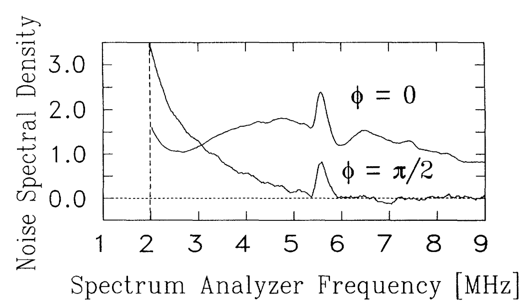

FIG. 2. Measured optical noise spectra for coherently driven two-level atoms. In-phase ($\phi = 0$) and out-of-phase ($\phi = \pi/2$) noise spectra are shown for the effective pulse area $\theta_M = 4\pi$. The noise spectral density has been divided by the measured shot noise spectral density (V^2/Hz) for 1 mW of total power; a noise spectral density of 0 corresponds to the shot noise level of the total transmitted power, which has been subtracted. Note that the small peak near 6 MHz is due to the ion laser.

equations for the independent two-level atoms. The calculated spectrum is written in terms of distinct noise sources as

$$S(\nu) = \eta_S\Big[P + \dot{N}\hbar\omega\left(\frac{P_{\rm LO}}{2P_x}\right)\frac{\eta_0}{4}\,\theta_M^2 \times \{[F_D(\nu) + F_{\rm SP}(\nu)] + [F_D(\nu) + F_B(\nu)]\cos2\phi\}\Big]. \qquad (1)$$

The first term in Eq. (1) is the mean square shot noise due to the total (both regions) transmitted power P. The terms $\propto\dot{N}\hbar\omega$ are the atom noise contributions, as described below. The rate $\dot{N}$ at which atoms cross each interaction region is determined by measuring the total phase-dependent power absorbed from the local oscillator. In Eq. (1), ν ($\Delta\nu$) is the spectrum analyzer frequency (bandwidth) in Hz. $\eta_S \equiv 2\hbar\omega\eta_0\Delta\nu$, with η_0 the detection system efficiency. $P_{\rm LO}$ (P_x) is the total transmitted (driving) field power with the laser fields off resonance. The maximum Bloch angle is $\theta_M = \Omega_R\tau\sqrt{\pi}$. The Rabi frequency Ω_R of the driving field and the transit time τ for atoms to cross an interaction region determine the frequency scales of the dimensionless spectral functions $F_D(\nu)$, etc.

We find $F_D(\nu) = F[\sin\theta, \sin\theta; \nu]$, $F_{\rm SP}(\nu) = F[1 - \cos\theta, 1 - \cos\theta; \nu]$, and $F_B(\nu) = F[\cos\theta + 1, \cos\theta - 1; \nu]$. Here, $F[f(\theta), g(\theta); \nu] = 2\,{\rm Re}\int_0^\infty d\tilde{\tau}\, e^{-i2\pi\nu\tau\tilde{\tau}} \times C[f(\theta), g(\theta); \tilde{\tau}]$, where the (normal and time ordered) correlation functions are

$$C[f(\theta), g(\theta); \tilde{\tau}] = \int_{-\infty}^{\infty}\frac{d\eta}{\sqrt{\pi}}\,e^{-2\eta^2} \times \int_{-\infty}^{\infty}\frac{d\xi}{\pi}\,e^{-(\xi+\tilde{\tau})^2-\xi^2} f[\theta(\xi + \tilde{\tau}, \eta)]\,g[\theta(\xi, \eta)]. \qquad (2)$$

In Eq. (2), the position-dependent Bloch angle is $\theta(\xi, \eta) = \theta_M \exp(-\eta^2)\,[1 + {\rm erf}(\xi)]/2$.

Three distinct sources of the atomic noise appear in Eq. (1): mean dipole Poisson noise F_D, mean square spontaneous emission noise $F_{\rm SP}$, and the phase-dependent part of the Bloch vector projection noise F_B. These are shown individually in Fig. 3(a), and are physically interpreted below, using the Bloch vector picture.

The $F_D(\nu)$ term arises from the mean dipole moment for each of the moving atoms. Each dipole that crosses the interaction region produces a pulse of absorption (or gain) in the transmitted power $\propto \sin\theta\cos\phi$. Here, θ is the position-dependent Bloch angle (time dependent in the atom frame) and ϕ is the fixed relative phase between the local oscillator and driving laser fields. The random occurrences of absorption cause phase-dependent Poisson noise, i.e., the number of radiating atoms is fluctuating. For N atoms, the mean square fluctuation in the transmitted power is proportional to $N\sin^2\theta\,\cos^2\phi$; this corresponds to $F_D(\nu)[1 + \cos2\phi]$ in Eq. (1). $F_D(\nu)$ is just the power spectrum of the product of $\sin\theta$ with the Gaussian distribution of the local oscillator field, i.e., $f = g = \sin\theta$ in Eq. (2). Similarly, spontaneous emission from the fluctuating part of the dipole causes a mean square fluctuation in the transmitted power. The corresponding spectrum $F_{\rm SP}(\nu)$ is determined by the excited state probability, with $f = g = 1 - \cos\theta$ [15]. We note that separating F_D from $F_{\rm SP}$ (or from F_B) is somewhat arbitrary, as only the combination is directly measurable in the experiments (see Robinson and Berman [15]).

The term $F_B(\nu)\cos2\phi$ arises from phase-dependent fluctuations in the projections of the Bloch vector, as explored theoretically by Wódkiewicz and Eberly [16]. This projection noise is analogous to the fluctuation of the spatial components of a spin vector which causes nuclear spin noise [17] and population fluctuations [18]. The role of Bloch vector projection noise in the present experiments can be understood as follows. When the Bloch vector is rotated to an angle θ by the driving field, the component which radiates in phase with the driving field has a mean square fluctuation $N\cos^2\theta$. This causes a mean square fluctuation in the transmitted power $\propto N\cos^2\theta\cos^2\phi$. The out-of-phase contribution, which is unaffected by the Bloch angle, varies as $N\sin^2\phi$. The net phase-dependent part of the projection noise from these two contributions is then $\propto N(\cos^2\theta - 1)\cos2\phi$. It follows that the spectrum $F_B(\nu)$ is determined by the negative correlation between absorption and emission, i.e., $f = 1 + \cos\theta$ and $g = -(1 - \cos\theta)$ in Eq. (2).

The measured dipole noise spectra can be compared to those calculated from Eq. (1). For the experiments, $P_x = 1.0$ mW (one region) and the maximum pulse area $\theta_M = 4\pi$. $\dot{N}\hbar\omega$ is determined to be $\simeq 0.35$ mW from the measured ϕ-dependent absorption of the transmitted total power. The power in the $\mathbf{z}$-polarized field for each interaction region is $P_z = 2.0$ mW. The detection system efficiency is $\eta_0 = 0.51$, as determined from the photocurrent conversion factor of $\eta_0 e/\hbar\omega = 0.23$ A/W. The spectrum analyzer bandwidth is $\Delta\nu = 100$ kHz. The $1/e$ field radii of the interaction regions are found to be $a = 100\ \mu$m, $b = 0.76$ mm. $v = 6 \times 10^4$ cm/sec is the supersonic speed, measured by time-of-flight methods, and $\tau = 0.17\ \mu$s.

Figure 3(b) shows the dipole noise spectral density $[S(\nu) - \eta_S P]/\eta_S$ in units of the shot noise spectral density for 1 mW. The spectra were calculated from Eq. (1) using the experimentally determined parameters. Both the predictions and the data (Fig. 2) have been divided by the factor $P_{\rm LO}/2P_x$, the ratio of the phase-dependent local oscillator power to the driving field power.

The observed spectra have a shape and approximate magnitude in good agreement with the predictions. For the in-phase spectrum, the broad peak centered near the Rabi sidebands arises from three sources: Spontaneous emission noise ($F_{\rm SP}$) and phase-dependent projection noise (F_B) add to contribute half of the amplitude, while the phase-dependent and phase-independent parts of the mean dipole Poisson noise (F_D) contribute the other half. Note that the mean dipole moment does not have an "elastic" in-phase peak, centered near zero frequency, as is the case for short-lived atoms [6]. For the long-lived atoms used in this experiment, the mean dipole moment is modulated at the Rabi frequency and the noise spectral function $F_D(\nu)$ is centered in the Rabi sidebands. For the out-of-phase spectrum, the mean dipole moment does not contribute, and F_{SP} and F_B subtract to produce the central peak.

As noted above, at a frequency of 3 MHz, the in-phase and out-of-phase noise components are of equal magnitude and the phase-dependent noise contribution vanishes. In this case, the mean dipole noise increases the net noise level by exactly the same amount that the phase-dependent projection noise decreases it. It is interesting to note that in a system with a prepared Bloch vector where θ is constant, the net phase-dependent noise contribution to the spectrum vanishes for all ν.

We note that there are some discrepancies between the measured and predicted spectra. The widths of the measured spectra are larger, and the amplitude of the measured in-phase peak is smaller, than predicted. The larger spectral widths cause the measured spectra to cross at a higher frequency, and to approach the shot noise level more slowly, than predicted. We believe that the larger spectral widths arise from imperfect magnetic compensation of the Doppler broadening in the experiments. Imperfect compensation leads to a range of generalized Rabi frequencies, which broadens the spectra and reduces the maximum amplitude of the noise signals.

In conclusion, we have measured phase-dependent noise spectra for the optical field radiated by long-lived two-level atoms in an atomic beam. By analyzing the spectra of this simple radiating system, it has been possible to understand in physical terms some interesting features of the phase-dependent noise spectra. We believe that the techniques employed in the measurements can be used to study noise in the radiation fields of atoms in a variety of configurations. These include atoms in dense Doppler compensated beams, in optical force fields, and in traps or cavities, where the mechanical effects of the light influence the atomic motion [19,20].

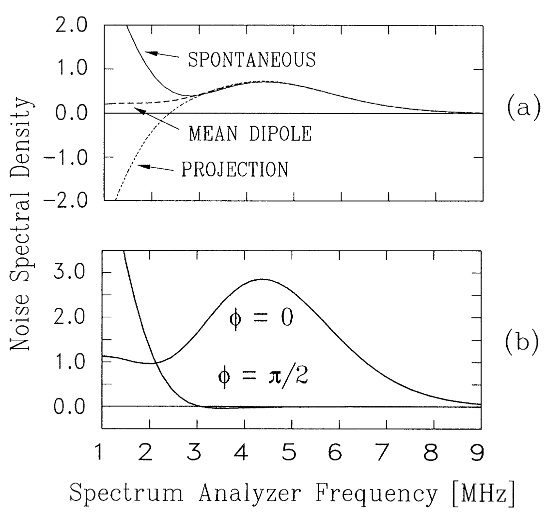

FIG. 3. (a) Atom noise spectral contributions for $\theta_M = 4\pi$: Mean dipole Poisson noise, dashed line; mean square spontaneous emission noise, solid line; phase-dependent Bloch vector projection noise, dotted line. (b) Calculated optical dipole noise spectra using no free parameters. In-phase quadrature, $\phi = 0$. Out-of-phase quadrature, $\phi = \pi/2$. Spectral density units as in Fig. 2.

This work has been supported in part by the National Science Foundation, the Rome Air Development Center, the Air Force Office of Sponsored Research, and the Army Research Office.

*Permanent address: Institute for Development of Advanced Technology, General Atomics, P.O. Box 85608, San Diego, CA 92186-9784.

[1] D. J. Wineland *et al.,* Phys. Rev. A **50**, 67 (1994).
[2] J. P. Gordon and A. Ashkin, Phys. Rev. A **21**, 1606 (1980); J. Dalibard and C. Cohen-Tannoudji, J. Opt. Soc. Am. B **2**, 1707 (1985).
[3] M. D. Reid and D. F. Walls, Phys. Rev. A **31**, 1622 (1985); A. Heidmann and S. Reynaud, J. Phys. **46**, 1937 (1985).
[4] R. E. Slusher *et al.,* Phys. Rev. Lett. **55**, 240 (1985); M. Maeda *et al.,* J. Opt. Soc. Am. B **4**, 1501 (1987); L. A. Orozco *et al., ibid.* **4**, 1490 (1987); M. Vallet *et al.,* Europhys. Lett. **11**, 739 (1990); D. M. Hope *et al.,* Phys. Rev. A **46**, R1181 (1992).
[5] For a recent review of optical noise, see S. Reynaud *et al.,* in *Progress in Quantum Optics XXX,* edited by E. Wolf (Elsevier, New York, 1992).
[6] See C. Cohen-Tannoudji, in *Frontiers in Laser Spectroscopy,* edited by R. Balian, S. Haroche, and S. Liberman (North-Holland, New York, 1977), Vol. 1, pp. 3–104.
[7] H.-A. Bachor and D. E. McClelland, Phys. Scr. **T40**, 40 (1991).
[8] M. Kauranen *et al.,* Phys. Rev. A **50**, R929 (1994).
[9] C. Schnurr *et al.,* Opt. Lett. **15**, 1997 (1990); K. D. Stokes *et al., ibid.* **14**, 1324 (1989).
[10] J. H. Shapiro, IEEE J. Quantum Electron. **21**, 237 (1985).
[11] H. P. Yuen and V. W. S. Chan, Opt. Lett. **8**, 177 (1983).
[12] Similar methods have been used previously. See G. L. Abbas *et al.,* IEEE J. Lightwave Tech. **3**, 1110 (1985).
[13] A. M. Bacon *et al.* (to be published).
[14] B. R. Mollow, Phys. Rev. **188**, 1969 (1969).
[15] Spectra similar to F_D and F_{SP} (without the Gaussian factor for the local oscillator) have been discussed in studies of fluorescence for two-level atoms driven by pulses short compared to the radiative lifetime. See K. Rzazewski and M. Florjanczyk, J. Phys. B **17**, L509 (1984); E. J. Robinson and P. R. Berman, *ibid.* **17**, L847 (1984); S. Cavalieri *et al., ibid.* **20**, 5363 (1987); M. Lewenstein *et al.,* J. Opt. Soc. Am. B **3**, 22 (1986); T.-S. Ho and H. Rabitz, Phys. Rev. A **37**, 4184 (1988).
[16] B. Wódkiewicz and J. H. Eberly, J. Opt. Soc. Am. B **2**, 458 (1985).
[17] T. Sleator *et al.,* Phys. Rev. Lett. **55**, 1742 (1985).
[18] W. M. Itano *et al.,* Phys. Rev. A **47**, 3554 (1993).
[19] C. I. Westbrook *et al.,* Phys. Rev. Lett. **65**, 33 (1990).
[20] R. Quadt *et al.,* Phys. Rev. Lett. **74**, 351 (1995).